



Computational Investigation of Pitch Motion of a High-Speed Craft Incorporated with Trim-Tabs

Ahmad Fitriadhy^{1,*}, Loke Yan Pheng², Iqmal Nor Hakim Adzh², Faisal Mahmuddin³, Anuar Abu Bakar¹, Mohd Azlan Musa², Mohd Sofiyen Sulaiman⁴

¹ Programme of Naval Architecture, Faculty of Ocean Engineering, Technology, and Informatics, University Malaysia Terengganu, Terengganu, Malaysia

² Programme of Maritime Technology, Faculty of Ocean Engineering, Technology, and Informatics, University Malaysia Terengganu, Terengganu, Malaysia

³ Department of Marine Engineering, Engineering Faculty, Hasanuddin University Jalan Perintis Kemerdekaan km. 10, Tamalanrea, Makassar, Indonesia

⁴ Programme of Environmental Technology, Faculty of Ocean Engineering, Technology, and Informatics, University Malaysia Terengganu, Terengganu, Malaysia

ARTICLE INFO

Article history:

Received 24 March 2022

Received in revised form 8 June 2022

Accepted 9 June 2022

Available online 30 June 2022

Keywords:

Computational Fluid Dynamic (CFD); Trim-Tabs; Pitch Motion; Froude Number; Angle of Trim-Tabs

ABSTRACT

An excessive trim by stern on a high-speed craft is vulnerable to decrease comfortable ride incorporated with the large pitch motion. To prevent such problem, the craft is then equipped with a device known as “trim-tabs” providing a lift force at the stern region, which leads to reduce pitch angle/trim of the craft. This paper presents computational modelling of trim-tabs on high-speed craft towards reducing the pitch motion in the calm water condition. Here, the commercial Computational Fluid Dynamic (CFD) software; called Numeca Fine Marine has been accordingly utilised to evaluate several effects of Froude numbers (Fr) and angle of the trim-tabs into characteristics of the lift force of the high-speed craft. The results revealed that the pitch motion of the high-speed craft equipped with the trim-tabs (5°) has significantly reduced up to 76% at $Fr = 1.0$. This can be explained that the installed trim-tabs has increased the negative trim moment, which inherently creates the restoring moment pushing the stern up along the pitch-axis. Meanwhile, this may cause involuntary the total ship's resistance increased. In general, this simulation pointed out the advantage of the trim-tabs to increase the comfortability of the high-speed craft.

1. Introduction

Military small craft is basically designed and utilized for multi-purpose such as coastal border protection, search and rescue duties. Typically, this craft is operated for high speeds condition. However, the craft may prompt to excessively trim by stern hull due to the significant difference in hydrodynamic pressure when a ship runs in head-seas with somewhat high-speed. Correspondingly, this high-speed craft has a certain possibility to suffer serious pitching motion, severe slamming and

* Corresponding author.

E-mail address: naoe.afit@gmail.com (Ahmad Fitriadhy)

<https://doi.org/10.37934/cfdl.14.6.5671>

dynamic instabilities due to high impact wave-loads. To resolve this problem, a trim-tabs model is then introduced, which connects to the end of the craft to control the trim by adjusting the angle of tab, relative to the larger surface, have been used to optimize the running trim of displacement, semi-planing, and planing vessels [1]. Geometrically, the trim tab has a simpler design as compared to hydrofoils model, which is mechanically easy to install. Merely, these trim-tabs or interceptor are utilized to control and stabilize the pitch angle of the craft while uphold the hydrodynamic flow characteristics surrounding the hull to a large extent.

In the past few years, several researchers have numerical and experimental investigations to evaluate the trim-tabs or interceptor on the pitch angle/trim performances of the high-speed craft. Avci and Barlas [2] conducted the experimental model test of three transverse locations of interceptors with six different deployment depths; they found that the trim angle reduced between 1.60° and 4.70° at Froude number within the range of $0.58 \leq Fr \leq 1.19$. Ghassemi *et al.*, [3] developed numerical method to find the optimum geometrical interceptor; the result revealed that the pressure variations have an effect on draft height and lifting forces which directly results in a better control of trim. In addition, Clement and Blount [4] conducted an experimental test and found that the high-speed boats with an optimized deflection angle show that if the planing hull is constructed and difficulties occur with the trim angles, the best way to save the hull is to use either a fixed or a controllable trim-tab. To maintain an efficient pitch angle behavior, the trim-tabs need to be accordingly adjusted with respect to the forward-speed as written by Savitsky and Brown [5]. Using numerical simulation approach, Ghadimi *et al.*, [6] reported that the high-speed craft equipped with the trim-tabs either fixed or controllable models demonstrated to reduce the trim angle incorporated with subsequent increase in the ship's total resistance. Meanwhile, Mansoori and Fernandes [1] found that integrated interceptor with trim tab showed better performance compared to an interceptor or a trim tab. Ertogan *et al.*, [7] investigated the linear parametric modelling using system identification methods and artificial neural network modelling to obtain the optimal trim controller. Jokar *et al.*, [8] found that the proper interceptor ratio d/h could control porpoising instability of the craft. Ikeda and Katayama [9] reported that trim variations may cause an increase in vessel resistance and create instabilities such as porpoising instability in the fast vessels. This instability involves periodic, coupled heave/pitch oscillations which may experience in a planing craft at high-speeds. Humphree [10] studied the effect of trim-tab on planing hulls and suggested that the basic principle of the interceptor trim-tab is to create pressure underneath the hull, at the stem of the boat. Therefore, for high-speed crafts, it is necessary to control the trim [11]. Following the previous works of Fitriadhy *et al.*, [12-15], the growing technologies of computers with high reliability and precision of codes for computational simulation, Computational Fluid Dynamic (CFD) approach has become attractive tool to investigate hydrodynamic lift force of the high-speed craft incorporated with the trim-tabs allowing to capture a fully hydrodynamic interaction surrounding the ship's hull. Apart the specific results, the computational is relatively, less time-consuming and even practical with flexibility parameter variations for various computational configurations.

This paper presents a CFD simulation to investigate pitch motion of a high-speed craft incorporated with trim-tabs model. Numeca FINE™/Marine CFD software is employed to assists in the study. As common CFD software, the incompressible unsteady Reynolds-Averaged Navier Stokes equations (RANSE) has been applied in which RANSE and continuity equations are discretized by the finite volume method based on Volume of Fluid (VOF) to deal with the nonlinear free surface. To achieve the research objective, several parameters such as effect of various Froude numbers and trim angle of the trim-tabs have been taken into account in the computational simulation. Here, the authors have set-up to release translation and rotational motions with respect to Z-axis (heave motion) and Y-axis (pitch motion). In addition to forward velocity, it has been appropriately imposed

to the ship's model according to the Froude numbers. The total ship's resistance and hydrodynamic lift forces are then quantified as relevant basis for assessing the pitch motion of the high-speed craft. Furthermore, the results described in this paper were displayed via CFD visualizations displaying properties of wave elevation, hydrodynamic pressure and turbulent viscosity. This is useful in providing an insight into the pitch motion characteristic of the high-speed craft from the hydrodynamic point of view. In the other words, it has led to effort being discussed to her pitch motion related to the aforementioned variable parameters as comprehensively explained in Section 3.

2. Methodology

2.1 Governing Equations

Basically, the current CFD flow solver is based on the incompressible unsteady RANSE, which means that finite volume is applied to the solver to build a spatial discretization of transport equation [16]. In addition, the velocity field is obtained from the momentum equations and the pressure field is extracted from the mass conservation constraint, or continuity equation, transformed into a pressure equation. The flow solver can deal with multi-phase flows and moving grids by integrating pressure and shear forces over the surface of a body.

2.2 Conservation Equations

In the multi-phase continuum, considering incompressible flow of viscous fluid under isothermal conditions, mass, momentum and volume fraction conservation equations can be expressed using the generalized form of Gauss' theorem as written by Fitriadhy and Adam [16].

2.3 Turbulent Model

In fluid dynamics, turbulent flow is characterized by chaotic property changes or by the random motion of fluid within a flow domain. Modeling transport and mixing by turbulence in complex flows is one of the greatest challenges for CFD [11]. Turbulent model is commonly presented in any flow and it is dominant over all other flow phenomena, an effective demonstrating of turbulence significantly increases the quality of numerical simulations [17]. In the selection of the turbulent model, the authors employ the SST k- ω (SST for shear-stress transport) model, which is able to improve the prediction of flows with strong adverse pressure gradients and separation. The set-up of the turbulent model was similar to the previous paper presented by Fitriadhy *et al.*, [12], which is then expressed in Eq. (1) and Eq. (2).

$$\frac{\partial \rho K}{\partial t} + \frac{\partial}{\partial x_j} \left(\rho U_j K - (\mu + \sigma_k \mu_t) \frac{\partial K}{\partial x_j} \right) = \tau_{ij} S_{ij} - \beta * \rho \omega K \quad (1)$$

$$\frac{\partial \rho \omega}{\partial t} + \frac{\partial}{\partial x_j} \left(\rho U_j \omega - (\mu + \sigma_\omega \mu_t) \frac{\partial \omega}{\partial x_j} \right) = P_\omega - \beta \rho \omega^2 + 2(1 - F_1) \frac{\rho \sigma_\omega^2}{\omega} \frac{\partial K}{\partial x_i} \frac{\partial \omega}{\partial x_j} \quad (2)$$

Identically, for wall-bounded and internal flows, the model gives good results only in cases where mean pressure gradients are small. Neither the k- ϵ model nor the k- ω model is suitable for flows with strong stream-wise vortices.

2.4 Principal Dimensions

The geometrical model of the high-speed craft is clearly shown in Figure 1. The principal data of her ship's particulars including the trim-tabs model are completely summarized in Table 1.

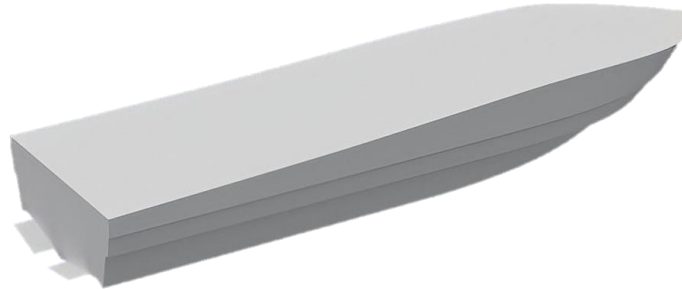


Fig. 1. Geometry of high-speed craft with trim-tabs model

Table 1
 Craft's particulars

Dimension	Value	
	w/o	Trim-Tabs
Length Between Perpendicular (m)	4.961	4.961
Breadth, B (m)	1.368	1.368
Draft (m)	0.2	0.2
Displacement Δ (Kg)	427.9487	428.068
Wetted Surface Area (WSA)	5.243	5.120
Chord (m)	-	0.230
Span (m)	-	0.301

2.5 Parametric Studies

To achieve the objective, several parameters such as the effect of Froude number within the range of 0.7 to 1.3 and various angle of trim-tabs have been employed in the simulation. The detailed simulation conditions are presented in Table 2 and Table 3 below.

Table 2
 Computational simulation conditions on Froude number

Description	Froude Number (Fr)						
	0.7	0.8	0.9	1.0	1.1	1.2	1.3
Total Resistance, R_T	√	√	√	√	√	√	√
Lift Force, F_L	√	√	√	√	√	√	√

Table 3
 Computational simulation condition on angle of trim-tabs

Description	α (deg)			
	0	1	3	5
Total Resistance, R_T	√	√	√	√
Lift Force, F_L	√	√	√	√

2.6 Computational Domain and Boundary Conditions

The computational domain and boundary conditions of the high-speed craft are summarized completely in Table 4. Each of the outside boundaries (inlet, outlet, side, top and bottom) are assigned as external (EXT) for velocity and pressure condition settings as clearly seen in Figure 2. In addition to the boundary of Y_{min} , it is defined as mirror, which is applied the symmetrical computational domain of the high-speed craft model to reduce the computational time. Here, the far-field conditions (X_{min} , X_{max} , and Y_{max}) are defined to initialize velocity, mass fraction and turbulence by insert a constant value along different directions. The conditions of Z_{max} and Z_{min} are defined as prescribed pressure to impose pressure during computation. The geometry of the high-speed craft incorporated with trim-tabs are assigned as solid patches. The domain's length with respect to the ship's position was specified to avoid reflection from the side and downstream boundary. The parameters of the computation simulation are defined based on the parametric studies and objectives. Two motions have been released with respect to the translation (heave) and rotation (pitch) motions about Z-axis and Y-axis, respectively. Meanwhile, the remaining four degrees of freedom were restrained.

Table 4
 Computational domain and boundary conditions

Description	Type	Condition
X_{min}	EXT	Far Field
X_{max}	EXT	Far Field
Z_{min}	EXT	Prescribed Pressure
Z_{max}	EXT	Prescribed Pressure
Y_{min}	MIR	Mirror
Y_{max}	EXT	Far Field

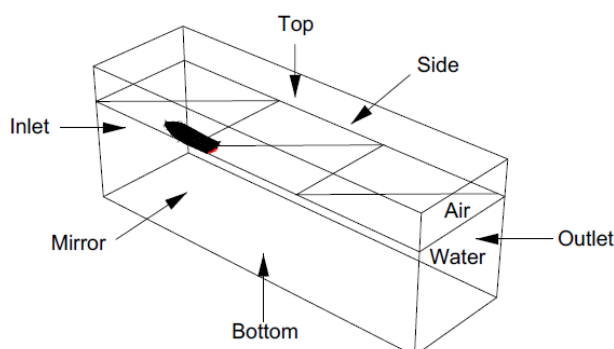


Fig. 2. Boundary condition

The mesh generation of the high-speed craft incorporated with the trim-tabs model has been created in the HEXPRESS™ module as displayed in Figure 3. The unstructured hexahedral meshes are employed in the meshing generation of the ship's model. The authors applied two different numbers of meshing models of meshing for the high-speed craft i.e., without and with the trim-tabs model, where the total meshing numbers are 1,809,131 and 2,345,371, respectively. To obtain a more reliable computational simulation, the mesh refinement around the trim-tabs model has been added. The dynamic fluid body interaction model was applied to compute the ship's motions both of translational motion and angular rotation due to acting fluid forces. The solver allows to compute the motions of a rigid body by integrating pressure and shear forces over the surface of a body.

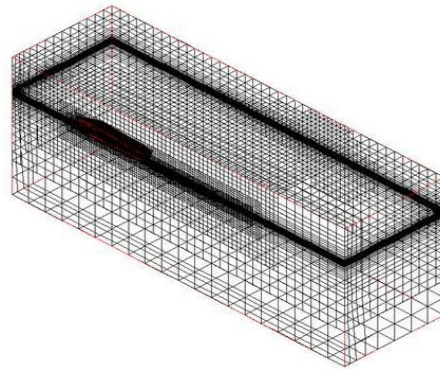


Fig. 3. Computational domain with unstructured hexahedral meshes

The example of the CFD simulation of the high-speed craft incorporated with the trim-tabs is shown in Figure 4, where the wave elevation, hydrodynamic pressure and turbulent viscosity are accordingly visualized.

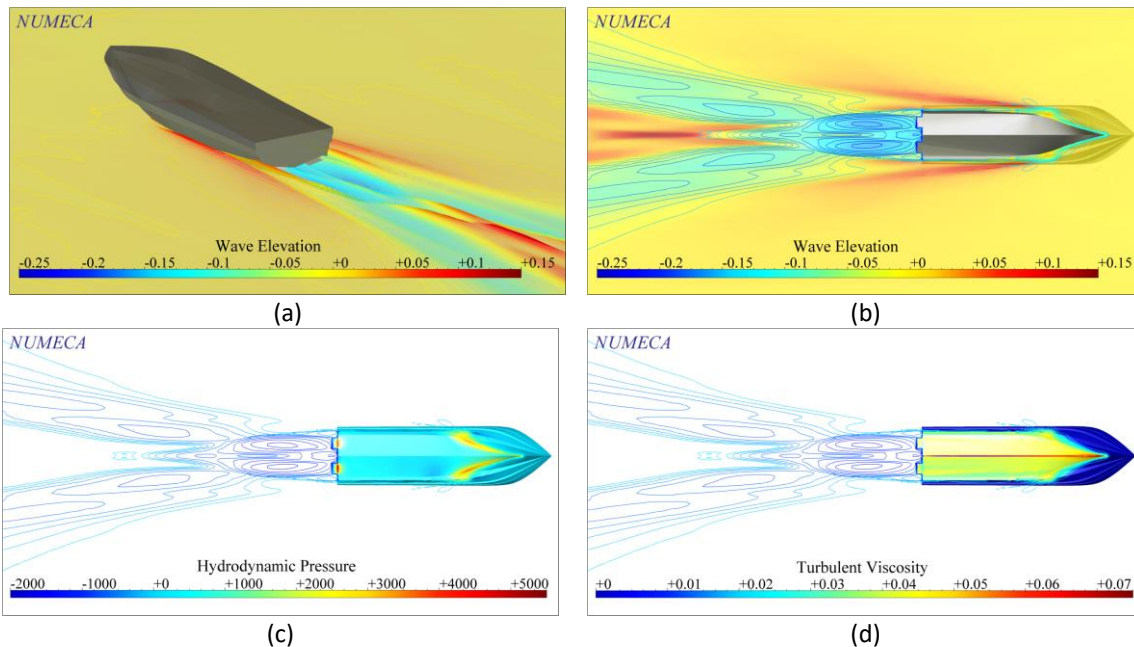


Fig. 4. Visualizations of wave elevations (a) and (b), hydrodynamic pressure (c) and turbulent viscosity (d) at $Fr = 1.3$ incorporated with trim-tabs model

3. Results and Discussion

3.1 Effect of Froude Number on Pitch Motion

The presence of the trim-tabs, it has generated a larger overturning moment at the stern region, which inherently decreased the pitch angle of the craft as clearly seen in Figure 5. This can be explained by the fact that the hydrodynamic lift force has led to push the stern up along the pitch-axis. Meanwhile, the vertical motion (heave motion) increased of the heave motion. It is noted that the $Fr = 1.0$ value resulted in the maximum reduction of the pitch motion by 76%; whilst the heave motion increased by 59%. These results showed that this coupling motion is strongly dependent on the Froude number and the hydrodynamic lift forces. However, the further increase of the forward velocity has been prone to reduce it, which performed into steady reduction of the pitch motions by 39% as completely summarized in Table 5. Here, the percentage of the pitch motion decrement has

quantitatively increased as well as the forward velocities increased. Similar to what was reported by vessels Mansoori and Fernandes [1], the effect of the trim-tabs has effectively provided restoring moment in which the craft opposed the unrestrained pitch motion (towards the negative trim angle) incorporated with the maximum heave motion. In the other word, the trim-tabs acted to control the pitch angle through converting the hydrodynamic lift forces against the trim moment, which could profound the negative trim of the craft. It is merely concluded that the increase of forward velocities has rendered different phenomena leading to increase the heave motion and inversely reduce the pitch motion of the high-speed craft regardless of the fact that this may lie beyond the total ship's resistance of the high-speed craft.

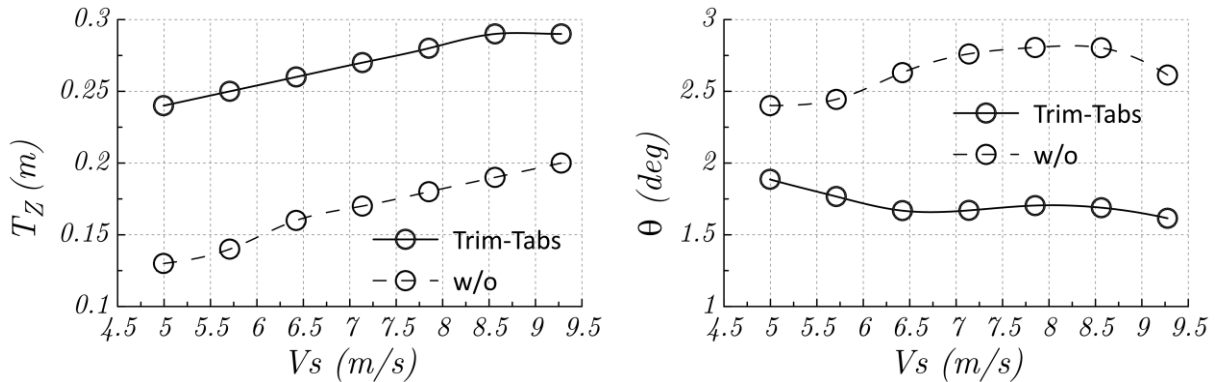


Fig. 5. Heave (left) and pitch (right) motions characteristics at various Froude numbers

Table 5

Heave and pitch motions characteristics at various Froude numbers

Fr	Vs (m/s)	Heave (m)		Pitch (deg)	
		w/o	Trim-Tabs	w/o	Trim-Tabs
0.7	4.995	0.13	0.24	2.401	1.886
0.8	5.708	0.14	0.25	2.444	1.767
0.9	6.422	0.16	0.26	2.631	1.668
1	7.136	0.17	0.27	2.761	1.670
1.1	7.85	0.18	0.28	2.806	1.704
1.2	8.563	0.19	0.29	2.803	1.689
1.3	9.277	0.20	0.29	2.614	1.615

The computational prediction of the total ship's resistance and the lift force of the high-speed craft without and with the trim-tabs (5°) are displayed in Figure 6. In general, the total ship's resistance was proportional to the increase of the forward velocity. As seen, the high-speed craft incorporated with the trim-tabs resulted in the higher total ship's resistance (R_T) as compared to the high-speed craft without the trim-tabs. This occurred mostly due to the stronger contribution of the larger wetted surface area, which is the basic function of R_T . It should be noted here that the effect of trim-tabs with respect to the total ship's resistance performances (R_T and C_T values) was insignificant at the lower speed. However, the value of R_T increased by 36% as the forward speed reached up to 9.277 m/s ($Fr = 1.3$) as presented in Table 6.

Table 6
 Total Resistance and coefficient of high-speed craft at various Froude numbers

Fr	Vs (m/s)	R _T (N)		C _T × 10 ⁻²	
		w/o	Trim-Tabs	w/o	Trim-Tabs
0.7	4.995	433.342	435.533	0.679	0.667
0.8	5.708	461.518	479.486	0.554	0.562
0.9	6.422	480.692	534.838	0.456	0.495
1	7.136	513.664	570.503	0.395	0.428
1.1	7.850	494.134	582.255	0.314	0.361
1.2	8.563	464.922	621.682	0.248	0.324
1.3	9.277	470.808	642.243	0.214	0.285

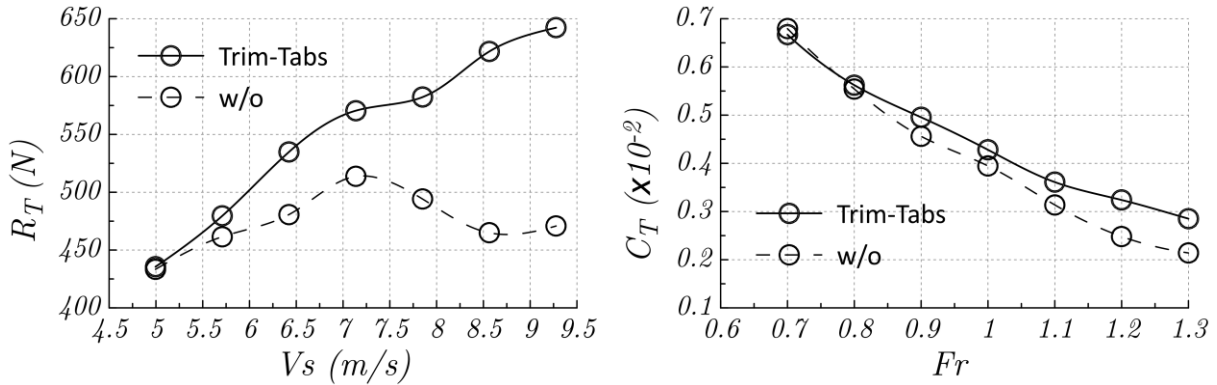


Fig. 6. Total resistance and coefficient characteristics of high-speed craft at various Froude numbers

In general, the magnitude of the lift force (F_L) and coefficient (C_L) for both conditions have similar trends with respect to the increase of the forward velocity, except at the condition of $Fr = 1.1$, as displayed in Figure 7. The detailed data of F_L and C_L are summarized in Table 7. However, the lift forces on the high-speed craft without the trim-tabs was insufficient to oppose the excessive pitch motion. This means that the lift force might not converted into the pitch restoring force. Meanwhile, the craft was resisted with the smaller heave motion with regards to her center of gravity. Thus, the ship will inevitably trim by stern.

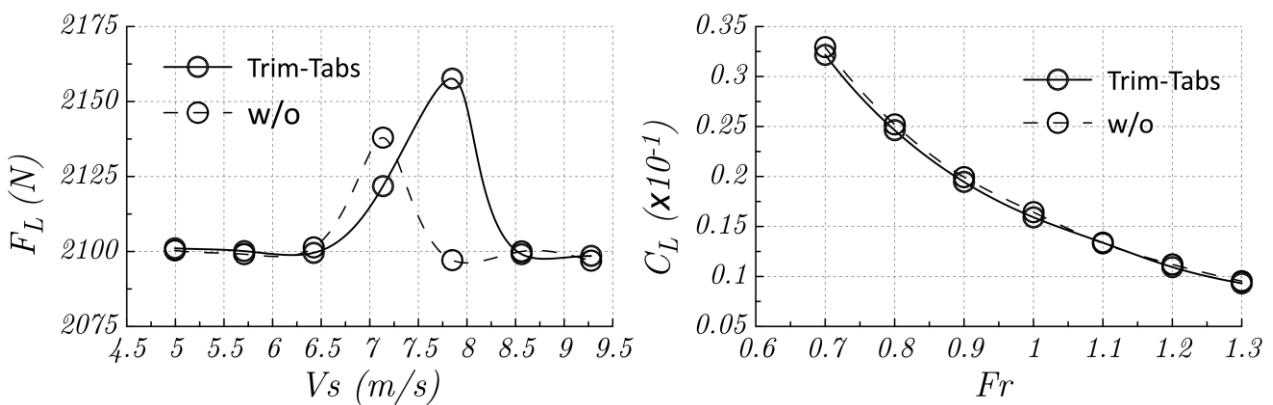


Fig. 7. Total resistance and coefficient characteristics of high-speed craft at various Froude numbers

Table 7
 Lift force and coefficient of high-speed craft at various Froude numbers

Fr	Vs (m/s)	F _L (N)		C _L × 10 ⁻¹	
		w/o	Trim-Tabs	w/o	Trim-Tabs
0.7	4.995	2100.347	2101.063	0.659	0.322
0.8	5.708	2099.087	2100.121	0.504	0.246
0.9	6.422	2101.317	2099.549	0.399	0.195
1	7.136	2137.914	2121.817	0.328	0.159
1.1	7.85	2097.08	2157.598	0.266	0.134
1.2	8.563	2100.013	2099.08	0.224	0.109
1.3	9.277	2096.964	2098.499	0.191	0.093

By referring to Figure 8 and Figure 9, the increase of the total ship’s resistance due to presence of the trim-tabs at three different of Froude numbers can be explained through the quantifying the wave elevation, the hydrodynamic pressure and the turbulent viscosity. The high-speed craft with the trim-tabs resulted in the higher wave elevation indicated with the existence of a higher wave crest (dark red color) in the forward region, which rose the total ship’s resistance. Meanwhile, this wave elevation area become larger heading towards the bow as seen in Figure 8(d) to Figure 8(f). This occurred mostly due to the overturning moment towards the bow as result of converting effectively the hydrodynamic lift forces at the stern part associated with the smaller pitch motion. Consequently, it exerted forcibly a hydrodynamic pressure field towards the bow of the craft; whilst the offset area of the turbulent viscosity become larger as displayed in Figure 9(d) to Figure 9(i), respectively. It can be concluded that the high-speed craft incorporated with the trim-tabs has suppressed the bow part which resulted in the higher total ship’s resistance as compared the high-speed craft without the trim-tabs.

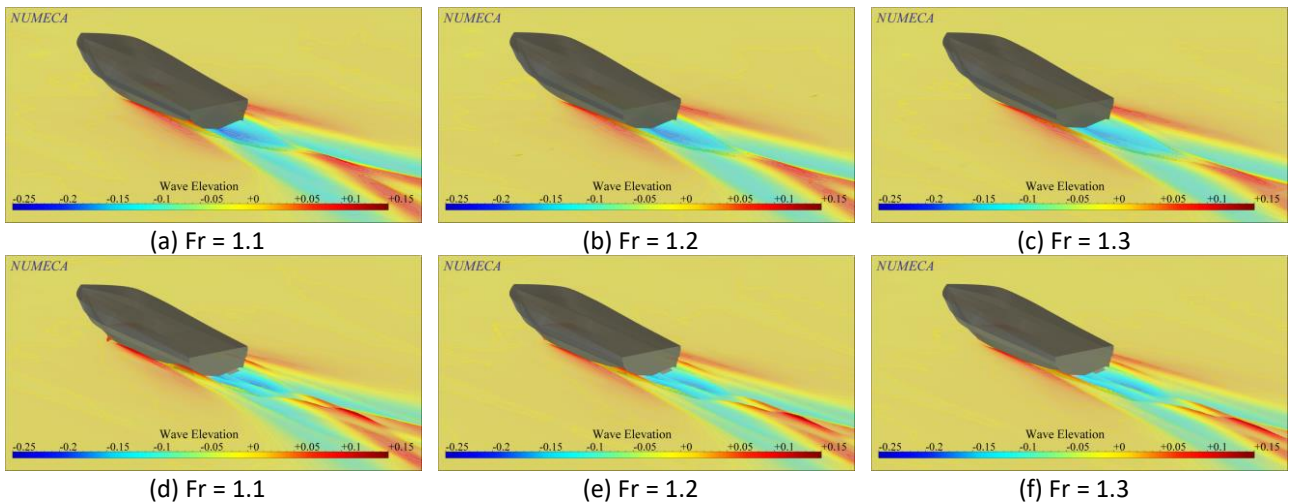


Fig. 8. 3D-wave elevation characteristics of high-speed craft without (above) and with trim-tabs of 5° model (below) at various Froude numbers

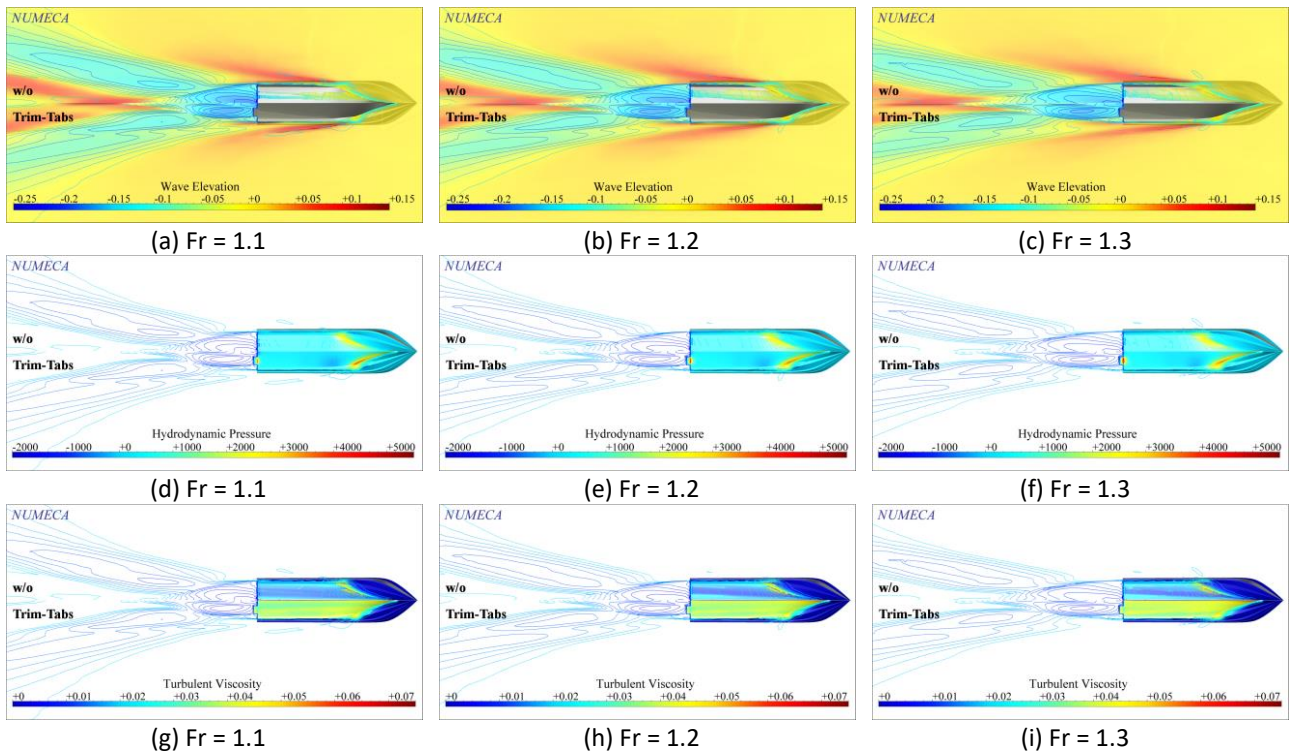
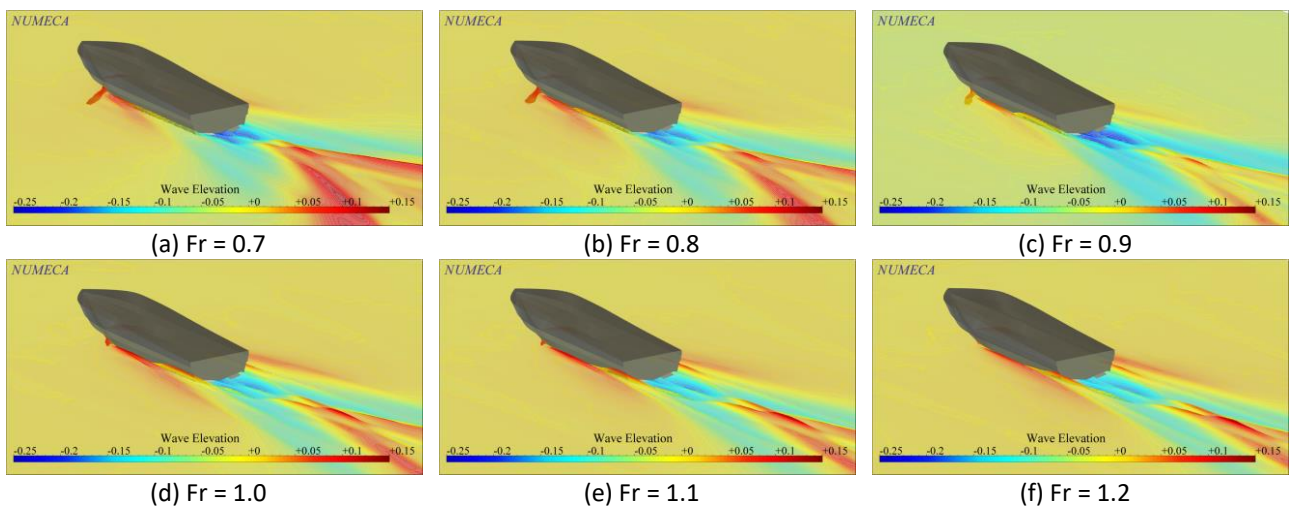
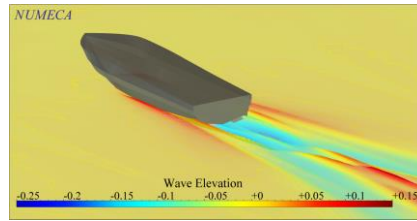


Fig. 9. 2D-wave elevation (top), hydrodynamic (middle) and turbulent viscosity (below) characteristics of high-speed craft without and with trim-tabs model (5°) at various Froude numbers

The characteristics of the wave elevation, the hydrodynamic pressure and the turbulent viscosity have been presented in Figure 10, Figure 11, Figure 12 and Figure 13, respectively. Similar to what was noted above, the CFD visualizations the high-speed craft have provided a meaningful answer to define the effect of the trim-tabs on the ship's resistance and the hydrodynamic lift forces related to the pitch motion performance of the high-speed craft incorporated with the trim-tabs. In this respect, it is interesting to note that the relationship between the Froude number and the hydrodynamic lift forces on the high-speed craft with the trim-tabs is seemingly non-linear appeared both in a qualitative and quantitative sense. Finally, it found that the vertical motions especially her pitch's angle has significantly reduced regardless of the Froude number increased (see Table 6).





(g) $Fr = 1.3$

Fig. 10. 3D-wave elevation, hydrodynamic and turbulent viscosity characteristics of high-speed craft without and with trim-tabs model (5°) at various Froude numbers

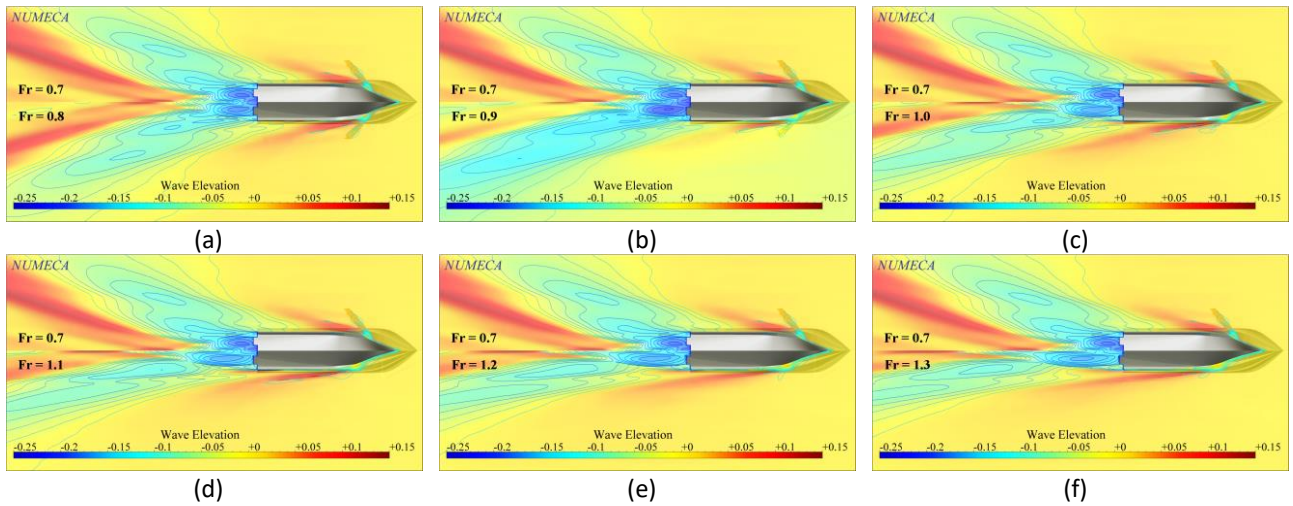


Fig. 11. 2D-wave elevation characteristics of high-speed craft incorporated with trim-tabs model (5°) at various Froude numbers

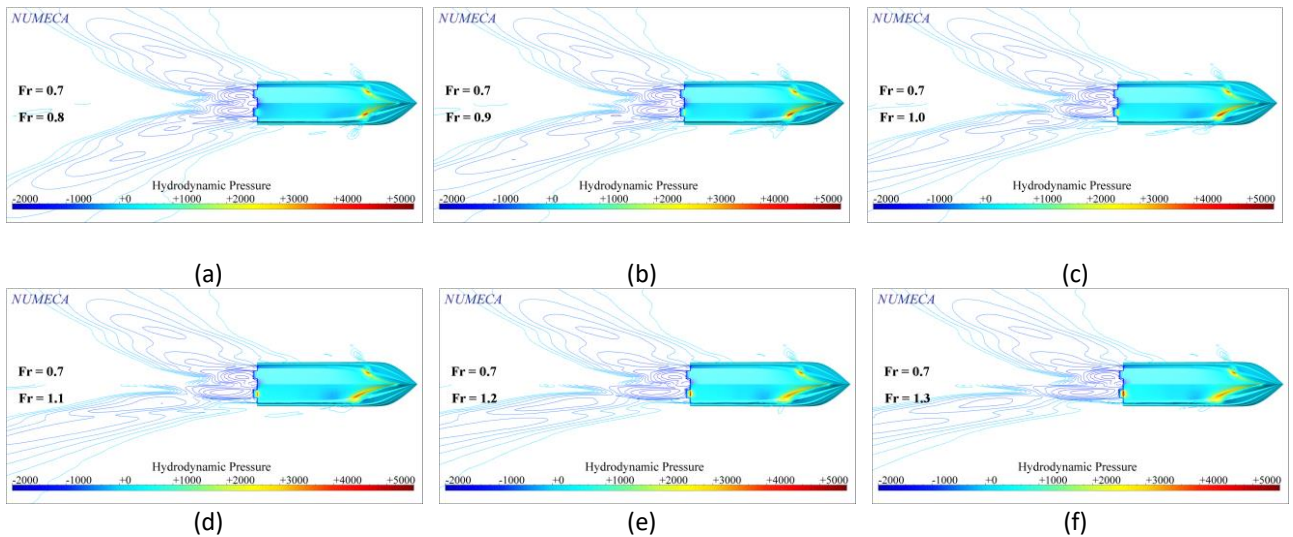


Fig. 12. Hydrodynamic characteristics of high-speed craft incorporated with trim-tabs model (5°) at various Froude numbers

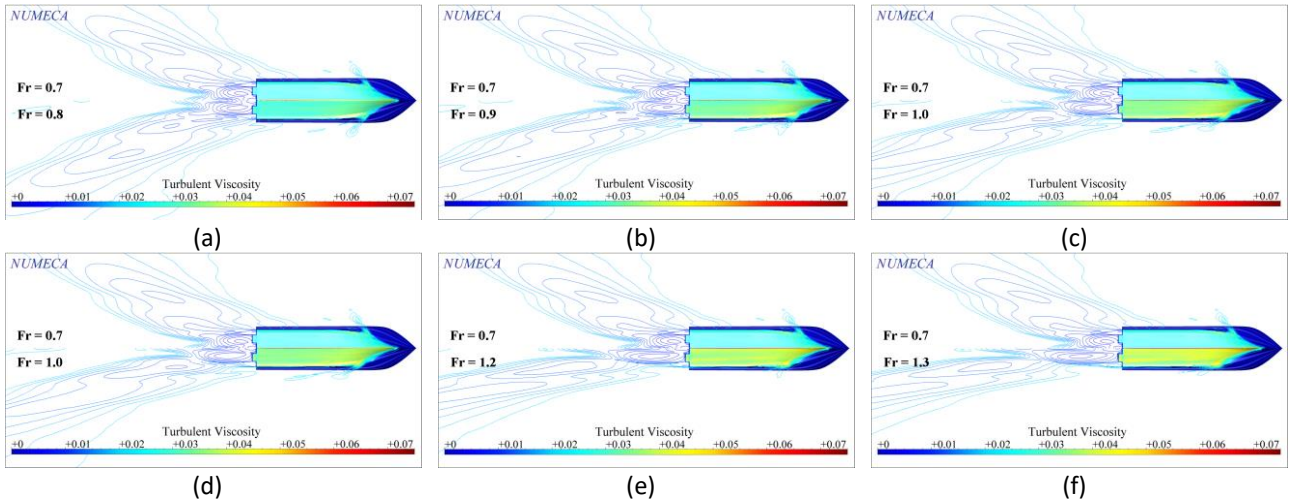


Fig. 13. Turbulent viscosity characteristics of high-speed craft incorporated with trim-tabs model (5°) at various Froude numbers

3.2 Effect of Trim-Tabs Angle

The effect of the trim-tabs angle on the vertical motions (heave and pitch motions) behaviour of the high-speed craft with constant speed has successfully assessed as shown in Figure 14. Although the heave motion was negligible small, the subsequent increase of the trim-tabs angle from 1°, 2° and 3° has brought about the valuable reduction of the pitch angle as presented in Table 8. It is noted that the pitch angle of the high-speed craft decreased by 14% and 27% as the trim-tabs angle increased from 1° to 2° and from 2° to 3°, respectively. As noted earlier, the reason helps to explain that the longitudinal buoyancy moved forward due to its centre of pressure is farther away from the initial axis of rotation to achieve the equilibrium condition is still water, where the pitch angle should be in the balance of the pitch moment acting on the submerge hull.

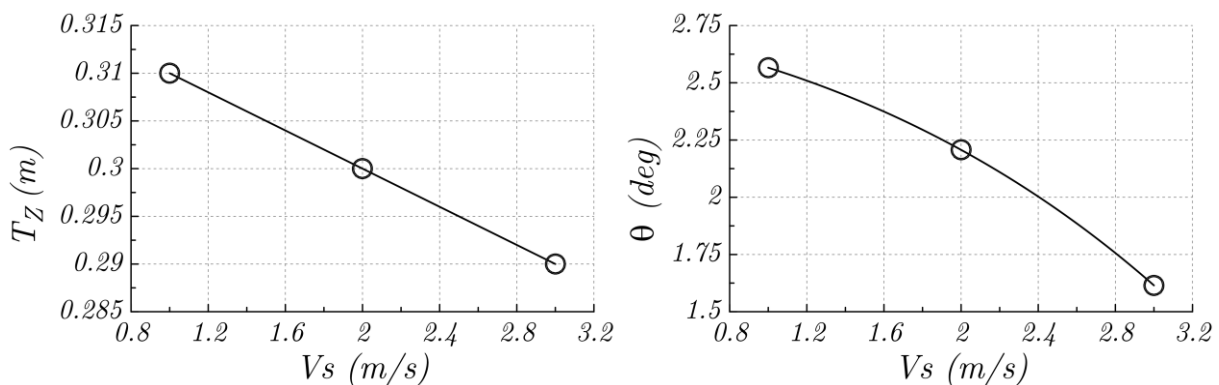


Fig. 14. Heave (left) and pitch (right) motions characteristics at various angles of trim-tabs

Table 8
 Heave and pitch motions characteristics at various angles of trim-tabs

α (deg)	Fr	V_s (m/s)	Heave (m)	Pitch (deg)
1	1.3	4.995	0.31	2.566
2	1.3	5.708	0.30	2.207
3	1.3	6.422	0.29	1.615

The total ship's resistance and the lift force of the high-speed craft have been displayed in Figure 15 and Figure 16. As noted before, the higher lift force was not fully converted into the hydrodynamic lift force to adjust the pitch attitude of the craft while under way indicated with the higher pitch angle. Merely, the values of R_T and F_L have included strong nonlinearities with respect to the trim-tabs angle as completely summarised in Table 8. Although the hydrodynamic of lift force is almost constant, the trim-tabs angle of 5° has the highest ship's resistance, which inversely proportional with the heave and pitch motions of the high-speed craft (see in Table 9). The reason behind this behaviour might be explained due to changing of the longitudinal center of pressure towards the stern of the craft. That is to say, the hydrodynamic lift force contributed to increase the wetted-surface area of high-speed craft that eventually resulted in to the increase of the total ship's resistance of high-speed craft.

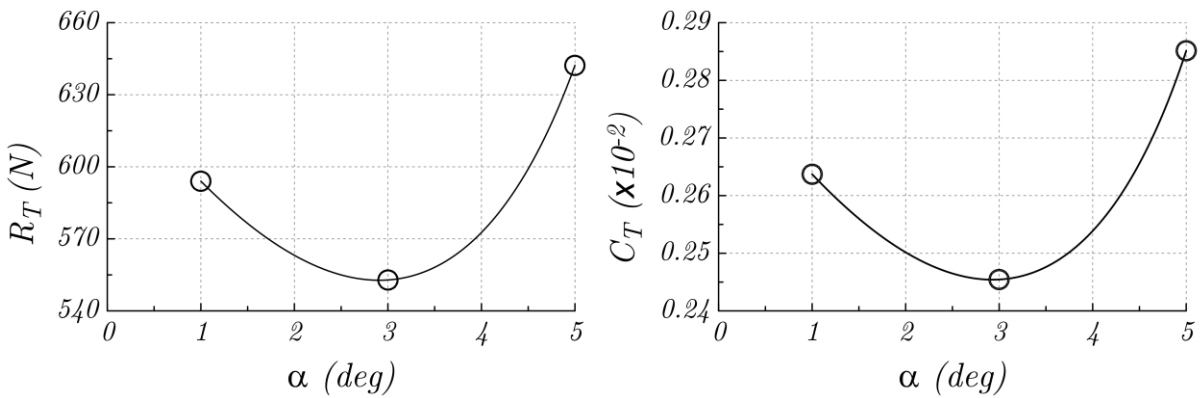


Fig. 15. Total resistance and coefficient at various angles of trim-tabs

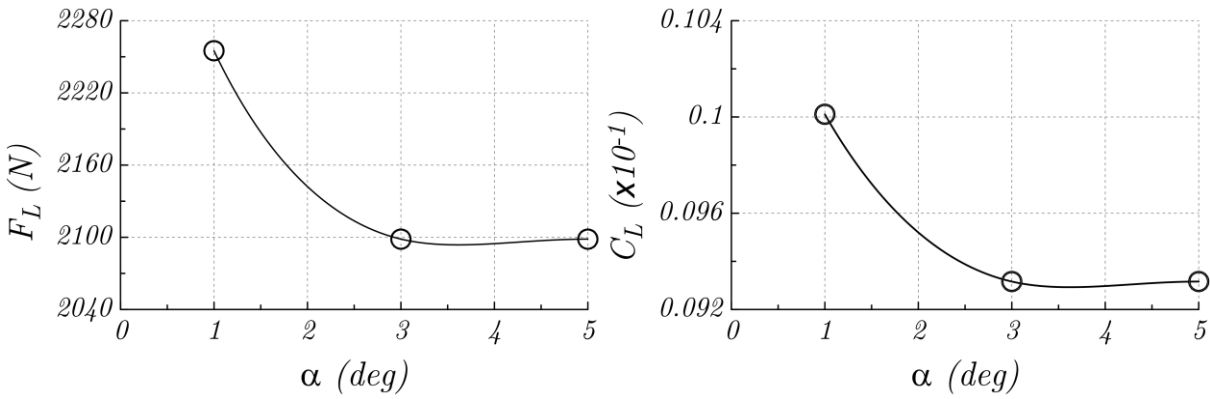


Fig. 16. Total resistance and coefficient at various angles of trim-tabs

Table 9

Resistance and lift forces characteristics at various angles of trim-tabs

α (deg)	R_T (N)	F_L (N)	$C_T \times (10^{-2})$	$C_L \times (10^{-1})$
1	594.018	2255.006	0.264	0.100
3	552.883	2098.520	0.245	0.093
5	642.243	2098.499	0.285	0.093

Referring to Figure 17 and Figure 18, the increase of the trim-tabs angle from 1° to 5° has considerably magnified the wave elevation surrounding the hull of the high-speed craft, which is proportional with increase of the water pressure behind the craft. This caused involuntary the total ship's resistance increased and change of heading exerted immense pressure would result in sufficient reduction of the pitch angle. Consequently, the craft initiated to trim by bow due to

converting of the hydrodynamic lift force into effective restoring force against trim moment towards the negative trim angle as well-explained in Sub-section 3.1. As seen in Figure 19 and Figure 20, the hydrodynamic pressure and the turbulent viscosity have been augmented.

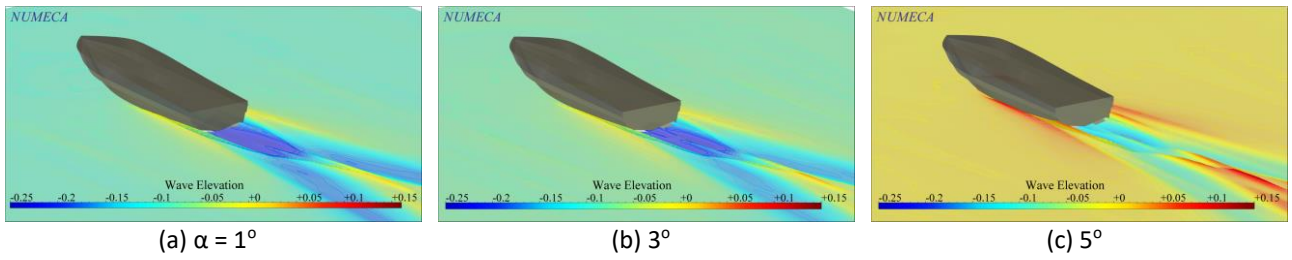


Fig. 17. 3D-wave elevation characteristics at various angle of trim-tabs

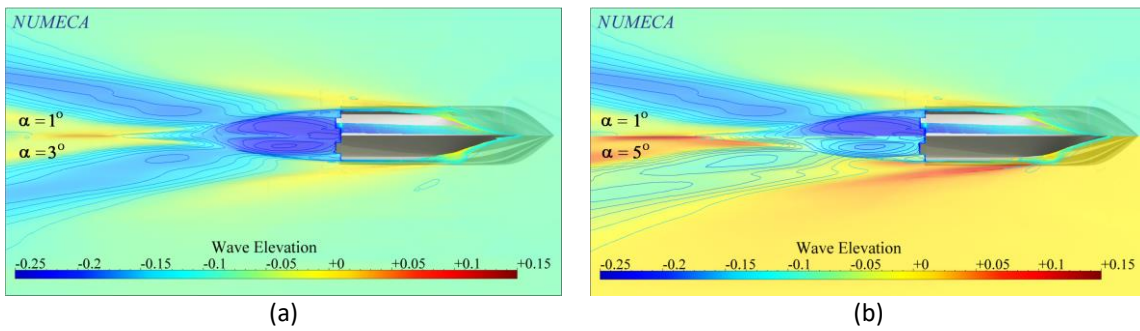


Fig. 18. 2D-wave elevation characteristics at various angle of trim-tabs

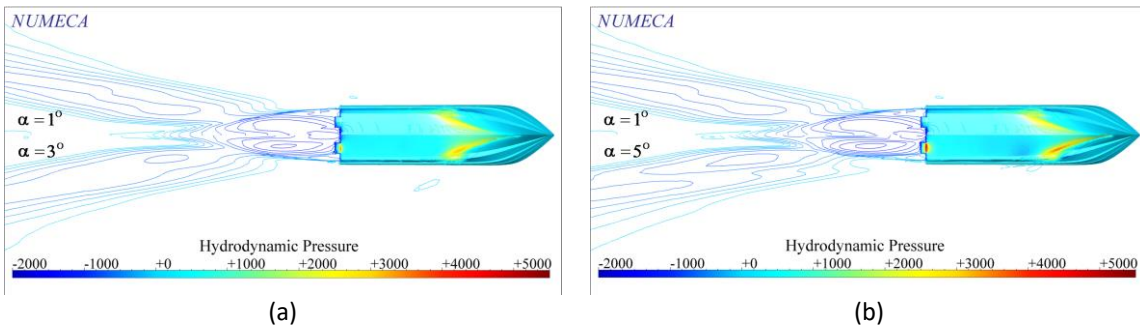


Fig. 19. Hydrodynamic characteristics at various angle of trim-tabs

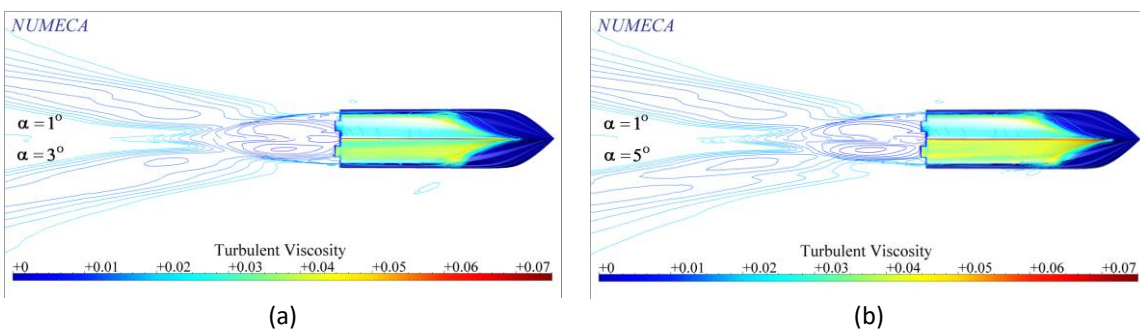


Fig. 20. Turbulent characteristics at various angle of trim-tabs

4. Conclusions

The computational investigation on predicting the pitch motion of the high-craft incorporated with the trim-tabs has successfully conducted. In this work, we aimed to obtain dynamic model behavior for pitch motion of a high-speed craft in the calm water. Here, The CFD approach has been

utilised in the simulation to provide an effective tool for investigating strongly nonlinear phenomena of the craft. The effect Froude numbers and angle of trim-tabs have been taken into account in the simulations. The results can be concluded as follow:

- i. The pitch motion has significantly reduced as well as the forward velocity increases due to presence of the hydrodynamic lift, which inherently creates the restoring moment pushing the stern up along the pitch-axis. It is worth to note that the maximum reduction of the pitch angle has reached up to 76% at $Fr = 1.0$.
- ii. In general, the high-speed craft with the trim-tabs resulted in the higher wave elevation indicated with the existence of a higher wave crest (dark red color) in the forward region, which inherently arise the total ship's resistance.
- iii. The subsequent increase of the trim-tabs angle has brought about the valuable reduction of the pitch angle by 14% and 27% as the trim-tabs angle increased from 1° to 2° and from 2° to 3° , respectively.
- iv. The total ship's resistance and the lift force have included strong nonlinearities with respect to the trim-tabs angle.

Acknowledgement

The authors wish to greatly thank Computer Simulation Laboratory, Department of Naval Architecture, Faculty of Ocean Engineering, Technology and Informatics, Universiti Malaysia Terengganu.

References

- [1] Mansoori, M., and A. C. Fernandes. "Interceptor and trim tab combination to prevent interceptor's unfit effects." *Ocean Engineering* 134 (2017): 140-156. <https://doi.org/10.1016/j.oceaneng.2017.02.024>
- [2] Avci, Ahmet Gultekin, and Baris Barlas. "An experimental investigation of interceptors for a high speed hull." *International Journal of Naval Architecture and Ocean Engineering* 11, no. 1 (2019): 256-273. <https://doi.org/10.1016/j.ijnaoe.2018.05.001>
- [3] Ghassemi, H., M. Mansouri, and S. Zaferanlouei. "Interceptor hydrodynamic analysis for handling trim control problems in the high-speed crafts." *Proceedings of the Institution of Mechanical Engineers, Part C: Journal of Mechanical Engineering Science* 225, no. 11 (2011): 2597-2618. <https://doi.org/10.1177/0954406211406650>
- [4] Clement, Eugene P., and Donald L. Blount. "Resistance tests of a systematic series of planing hull forms." *Trans. SNAME* 71, no. 3 (1963): 491-579.
- [5] Savitsky, Daniel, and P. Ward Brown. "Procedures for hydrodynamic evaluation of planing hulls in smooth and rough water." *Marine Technology and SNAME News* 13, no. 04 (1976): 381-400. <https://doi.org/10.5957/mt1.1976.13.4.381>
- [6] Ghadimi, Parviz, Afshin Loni, Hashem Nowruzi, Abbas Dashtimanesh, and Sasan Tavakoli. "Parametric study of the effects of trim tabs on running trim and resistance of planing hulls." *Advances in Shipping and Ocean Engineering* 3, no. 1 (2014): 1-12.
- [7] Ertogan, Melek, Philip A. Wilson, Gokhan Tansel Tayyar, and Seniz Ertugrul. "Optimal trim control of a high-speed craft by trim tabs/interceptors Part I: Pitch and surge coupled dynamic modelling using sea trial data." *Ocean Engineering* 130 (2017): 300-309. <https://doi.org/10.1016/j.oceaneng.2016.12.007>
- [8] Jokar, H., H. Zeinali, and M. H. Tamaddondar. "Planing craft control using pneumatically driven trim tab." *Mathematics and Computers in Simulation* 178 (2020): 439-463. <https://doi.org/10.1016/j.matcom.2020.05.032>
- [9] Ikeda, Yoshiho, and T. Katayama. "Stability of high speed craft." *Contemporary Ideas on Ship Stability* (2000): 401-409. <https://doi.org/10.1016/B978-008043652-4/50031-6>
- [10] Humphree. "Roll/Pitch Stabilization." *Humphree*. April, 2011. <https://humphree.com/functions/humphree-active-stabilization/>.
- [11] Xi, Handa, and Jing Sun. "Feedback stabilization of high-speed planing vessels by a controllable transom flap." *IEEE Journal of Oceanic Engineering* 31, no. 2 (2006): 421-431. <https://doi.org/10.1109/JOE.2006.875097>
- [12] Fitriadhy, A., M. A. Faiz, and S. F. Abdullah. "Computational fluid dynamics analysis of cylindrical floating breakwater towards reduction of sediment transport." *Journal of Mechanical Engineering and Sciences* 11, no. 4 (2017): 3072-3085. <https://doi.org/10.15282/jmes.11.4.2017.10.0276>

- [13] Fitriadhy, A., M. K. Aswad, N. Adlina Aldin, N. Aqilah Mansor, A. A. Bakar, and W. B. Wan Nik. "Computational fluid dynamics analysis on the course stability of a towed ship." *Journal of Mechanical Engineering and Sciences* 11, no. 3 (2017): 2919. <https://doi.org/10.15282/jmes.11.3.2017.12.0263>
- [14] Fitriadhy, Ahmad, Nur Adlina Aldin, and Nurul Aqilah Mansor. "CFD analysis on course stability of a towed ship incorporated with symmetrical bridle towline." *CFD Letters* 11, no. 12 (2019): 88-98.
- [15] Fitriadhy, A., N. Razali, and N. Aqilah Mansor. "Seakeeping performance of a rounded hull catamaran in waves using CFD approach." *Journal of Mechanical Engineering and Sciences* 11, no. 2 (2017): 2601-2614. <https://doi.org/10.15282/jmes.11.2.2017.4.0238>
- [16] Fitriadhy, A., and N. Amira Adam. "Heave and pitch motions performance of a monotriconic ship in head-seas." *International Journal of Automotive & Mechanical Engineering* 14, no. 2 (2017): 4243-4258. <https://doi.org/10.15282/ijame.14.2.2017.10.0339>
- [17] Sherbaz, Salma, and Wenyang Duan. "Ship trim optimization: assessment of influence of trim on resistance of MOERI container ship." *The Scientific World Journal* 2014 (2014). <https://doi.org/10.1155/2014/603695>